Environmental Science & Technology

Article

pubs.acs.org/est

In situ Imaging of Interfacial Precipitation of Phosphate on Goethite

Lijun Wang,*[,†] Christine V. Putnis,*[,‡,§] Encarnación Ruiz-Agudo,[∥] Jörn Hövelmann,[‡] and Andrew Putnis[‡,⊥]

[†]College of Resources and Environment, Huazhong Agricultural University, Wuhan 430070, China

[‡]Institut für Mineralogie, University of Münster, 48149 Münster, Germany

[§]Department of Chemistry, Curtin University, P.O. Box U1987, Perth, Washington 6845, Australia

[∥]Department of Mineralogy and Petrology, University of Granada, Granada 18071, Spain

[⊥]The Institute for Geoscience Research (TIGeR), Curtin University, Perth, Washington 6102, Australia

Supporting Information

ABSTRACT: Adsorption and subsequent immobilization of orthophosphate on iron oxides is of considerable importance in soil fertility and eutrophication studies. Here, in situ atomic force microscopy (AFM) has been used to probe the interaction of phosphate-bearing solutions with goethite, α-FeOOH, (010) cleavage surfaces. During the dissolution of goethite we observed simultaneous nucleation of nanoparticles (1.0−3.0 nm in height) of iron phosphate (Fe−P) phases at the earliest nucleation stages, subsequent aggregation to form secondary particles (about 6.0 nm in height) and layered precipitates under various pH values and ionic strengths relevant to acid soil solution conditions. The heterogeneous nucleation rates of Fe−P precipitates at phosphate concentrations ranging from 5.0 to 50.0 mM were quantitatively defined. Enhanced goethite dissolution in the presence of high concentration NaCl or $AlCl_3$ leads to a rapid increase in Fe−P nucleation rates, whereas low concentration $MgCl_2$ inhibits goethite dissolution, this in turn influences Fe−P nucleation. Moreover, kinetic data analyses show that low concentrations of citrate caused an increase in the nucleation rate of Fe−P phases. However, at higher concentrations of citrate, nucleation acceleration was reversed with much longer induction times to form Fe−P nuclei. These in situ observations may improve the mechanistic understanding of processes resulting in phosphate immobilization by goethite-rich acid soils in the presence of various inorganic and organic additive molecules.

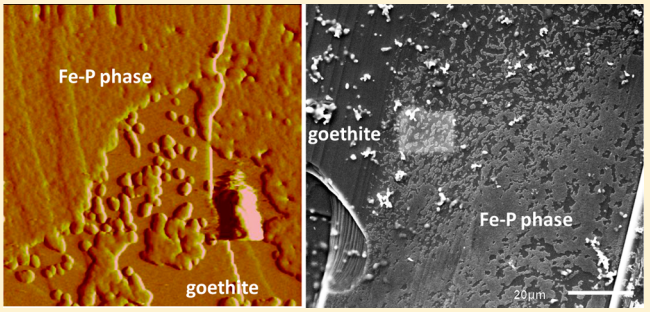

INTRODUCTION

Phosphorus (P) is a main limiting macronutrient for plant growth[1,2] and mineable resources of this essential nutrient are limited while, on the other hand, excess P, especially more soluble forms of orthophosphate leaching into water bodies is polluting our environment.[3,4] In addition to the potential for P-induced eutrophication, the unique problem is low P bioavailability in diverse alkaline and acid soils. In alkaline soils, the mobilization of phosphate in the soil environment is markedly influenced by calcite mineral surfaces, and that surface adsorption reaction and subsequent precipitation are major mechanisms of P immobilization,[5] lowering its bioavailability when dissolved P is added as a fertilizer. For acid surface soils, (hydr)oxides of iron (Fe) and aluminum (Al), albeit different in relative contribution, play key roles in phosphate sorption and precipitation.[6] On such soils, plants often show severe P deficiency symptoms and relatively large amounts of P fertilizer must be applied to meet plant requirements;[7] however, excess P in soil may increase the risk of P contamination through the migration and eutrophication of surface and underground waters and of phosphate-induced mobilization of arsenic, chromium, and other anionic contaminants.[8] Therefore, predicting the transformation, mobility and the inseparable link between the chemical species of phosphate may contribute to an improved understanding of the fate of dissolved phosphate species in diverse soil systems.

In this study, we chose goethite (α-FeOOH) because it has long been recognized as one of the most abundant of the naturally occurring iron oxides in soils. Although goethite may only make up 1−5% of the mineralogical composition of soil, goethite surfaces may account for 50−70% of the total surface area of the soil, both due to its fine grain size and its prevalence as a coating on other soil minerals.[9] Goethite has been widely used as a proxy and a representative iron oxide in P adsorption.[10,11] It is evident that phosphate interactions with iron oxides in natural soils are complex, and that multiple competitive and synergistic effects in pH dependent phosphate

Received: September 22, 2014
Revised: March 11, 2015
Accepted: March 12, 2015
Published: March 12, 2015

DOI: 10.1021/acs.est.5b00312
Environ. Sci. Technol. 2015, 49, 4184−4192

adsorption are widely present.[12] The relative paucity of available techniques has limited the progress toward an understanding of the chemistry of phosphate uptake on Fe oxides. Most studies focus on adsorption theory/modeling, and directly analyze the nature of the phosphate-oxide surface complexes. The main mechanisms include both nonspecific and specific adsorption.[13] In one of the earliest studies, Atkinson et al.[14] proposed that phosphate specifically replaces type A hydroxyl group and forms bridges between adjacent Fe^{3+}. Afterward, many adsorption models and surface complex formation models were unraveled:[15−24] Adsorption of orthophosphate on goethite mainly involves a ligand exchange mechanism, and three different types of complexes are present including protonated and nonprotonated bridging bidentate as well as a nonprotonated monodentate between orthophosphate ions and surface Fe^{3+} of α-FeOOH.[15] Rahnemaie et al. showed that various ligand models are dependent on the surface coverage and solution pH.[25] Recently, Kim et al.[26] demonstrated that the phosphate ions bind to the surface through two P−O−Fe linkages by ^{31}P NMR: the formation of innersphere complexes between phosphate and goethite surface and the presence of Fe^{3+}−O−P covalent bonds. In general, phosphates can form chemisorbed innersphere complexes via ligand exchange reactions between phosphate oxygens and hydroxyl oxygens of goethite,[27,28] and outersphere complexes via electrostatic interactions of phosphate anions with $Fe-OH_2^+$ groups may also be present. That is, no covalent Fe−O−P bonds are formed.[29]

In addition to surface adsorption, an alternative mechanism (i.e., another source for P uptake by iron oxides) is surface precipitation.[30,31] Ler and Stanforth confirmed the slow increase in ζ-potential of goethite after long-term reactions, indicating that this most likely involves the dissolution of goethite to release iron and the subsequent precipitation reaction between the iron and surface-bound phosphate.[32] Nooney et al.[33] first demonstrated initially rapid phosphate chemisorption, followed by island growth on a thin film of iron oxide when exposed to a sodium phosphate solution. While these results have suggested that the adsorption/surface precipitation process involves the dissolution of goethite,[32] details concerning the coupled dissolution and precipitation processes occurring during P adsorption on goethite remain unclear. Specifically, a direct observation of the kinetic pathways of precipitation at the goethite-phosphate solution interface at microscopic levels is lacking. In this study, we investigate, by in situ imaging, the Fe−P nucleation and subsequent growth on goethite surfaces using atomic force microscopy (AFM) coupled with a fluid reaction cell through which solutions with varying compositions relevant to acid soil solution conditions flowed. To our knowledge, there has been no experimental effort to directly measure the thermodynamic and kinetic contributions to the surface nucleation rates of Fe−P phases on goethite under chemical conditions that mimic natural phosphate precipitation environments. These direct observations may improve the mechanistic understanding of processes resulting in phosphate immobilization in diverse soil systems. The purpose of this study is to define the potential role of goethite surfaces in controlling phosphate precipitation at the nanoscale by probing the interaction of phosphate-bearing solutions with goethite (010) cleavage surfaces, using in situ atomic force microscopy (AFM).

EXPERIMENTAL SECTION

A natural goethite crystal (Michigan) was cleaved in order to expose a fresh cleavage (010) surface immediately prior to each in situ dissolution experiment, which was performed using a Digital Instruments (Bruker) Nanoscope IIIa AFM working in contact mode and equipped with a fluid cell. The collected AFM images using Si_3N_4 tips (Bruker, tip model NP-S10, spring constants of 0.12 N/m and 0.58 N/m) were analyzed using the NanoScope software (Version 5.31r1).

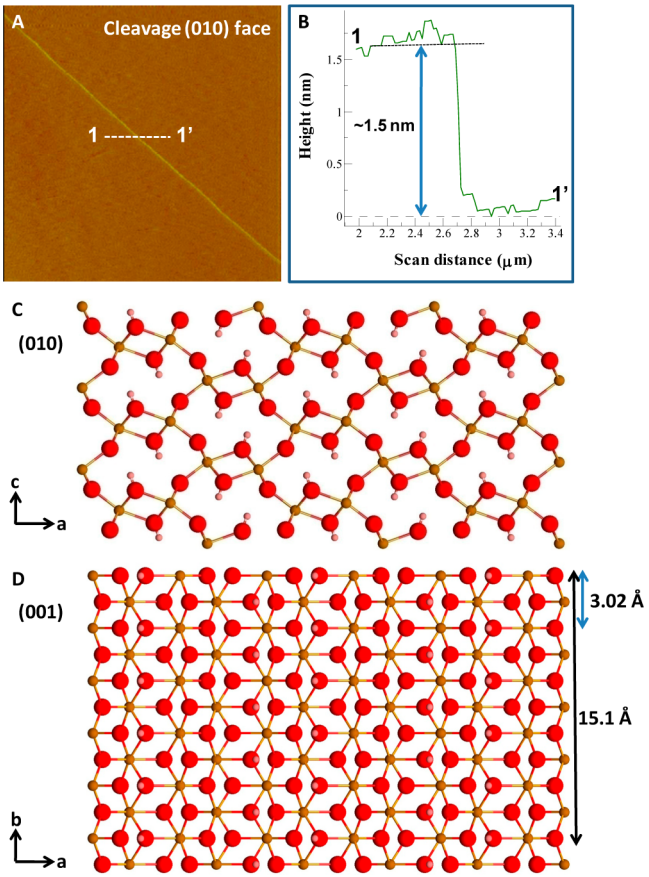

Figure 1. (A) AFM deflection image of a goethite (010) cleavage surface and (B) depth profile along line 1 → 1′ on the height image showing that the step height is close to 1.5 nm corresponding to the thickness of 5 unit cells along the *c* axis. (C) (010) and (D) (001) face of the goethite structure. Oxygen atoms are red, iron atoms are yellow, and hydrogen atoms are pink. Image A, 3 × 3 μm.

Ammonium dihydrogen phosphate (5−50 mM $NH_4H_2PO_4$, pH 4.5) solutions were passed through the fluid cell (2 mL per 1.5 min) in order to ensure surface-controlled reaction rather than diffusion control.[34] The pH values of $NH_4H_2PO_4$ solutions were adjusted to 6.0 using 0.01 M NaOH or pH 2.0 and 3.0 using 0.01 M HCl. NaCl, $AlCl_3$ or $MgCl_2$ at concentrations ranging from 10−500 mM was added to the phosphate solutions to investigate the effects of ionic strength and inorganic additives on goethite-phosphate interaction. In addition, the effect of an organic additive was studied by adding monosodium citrate (1−50 μM) to the phosphate solution. Nucleation rates of precipitated iron phosphate (Fe−P) were measured from particle density data collected shortly after the onset of precipitate formation, typically within the first 10−100 min at the earliest stages of nucleation. Different locations of

DOI: 10.1021/acs.est.5b00312
Environ. Sci. Technol. 2015, 49, 4184−4192

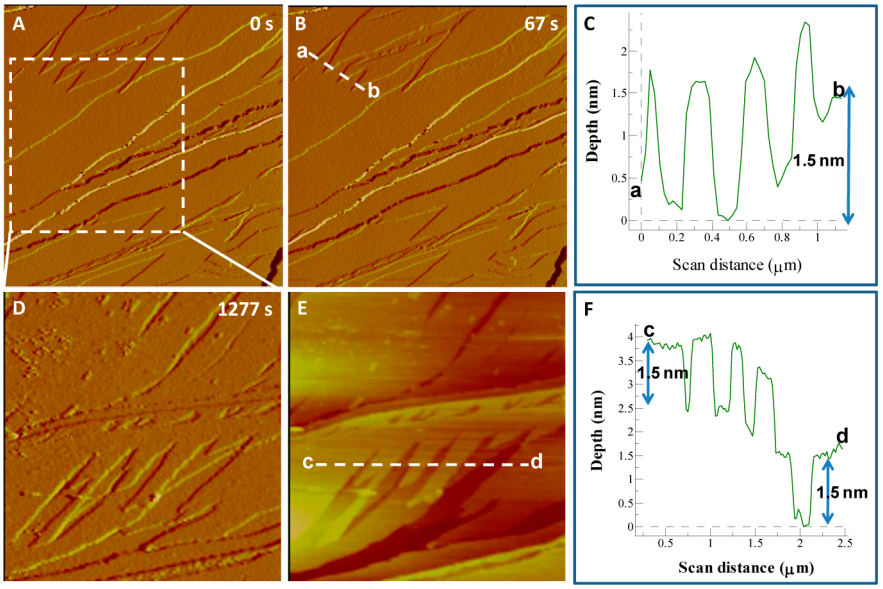

Figure 2. A sequence of AFM deflection images (A, B, D) and the height image of D (E) shows dissolution on the surface of a goethite crystal when exposed to the 5 mM $NH_4H_2PO_4$ solution at pH 4.5 at (A) t = 0 s, (B) 67 s and (D) 1227 s, respectively. (C, F) the cross-sectional analyses of the height (depth) of steps along dotted lines (a → b and c → d in B and E, respectively). A dotted rectangle in (A) shows the same area in (D) after about 21 min of injecting reaction phosphate solutions and the removal of steps with about 1.5 nm in depth (C, F) became evident on the dissolving goethite (010) surface. No etch pits were observed. Images A and B, 5 × 5 μm; D and E, 3 × 3 μm.

three different crystals per solution condition were imaged to ensure reproducibility of the results. All data with their mean values ± standard deviation (SD) of three independent experiments are presented.

Ex situ dissolution experiments (50 mM $NH_4H_2PO_4$, pH 4.5) were performed following in situ AFM experiments. The sample removed from the AFM fluid cell was placed in a beaker filled with ca. 10 mL of different solutions at room temperature. After 1−3 day reaction, the reacted crystal surface was carbon coated and observed in a scanning electron microscope (SEM, JEOL JSM 6460 LV) equipped with an energy dispersive X-ray (EDX) detector (Oxford Instruments) at an acceleration voltage of 20 keV for elemental analyses of newly formed precipitates on the goethite surfaces.

The PHREEQC modeling software[35] was used to calculate solution speciation in a volume of ca. 38 μL of phosphate-bearing solution in the AFM fluid cell in goethite dissolution experiments. This reaction was simulated by the addition of small increments of FeOOH to the solution until equilibrium with respect to goethite was reached. The saturation index (SI) of each solution with respect to the different Fe−P phases was calculated using the MINTEQ database when the solution was in equilibrium with respect to goethite. Based on our PHREEQC simulations, formation of a Fe−P phase on goethite surfaces under the AFM fluid cell conditions is thermodynamically favorable/possible. The relative supersaturation for a given Fe−P phase[36] including cacoxenite ($Fe_4(PO_4)_3(OH)_3{\cdot}12H_2O$), tinticite ($Fe_3(PO_4)_2(OH)_3{\cdot}3H_2O$), strengite ($FePO_4{\cdot}2H_2O$), or an Al−P phase, wavellite ($Al_3(PO_4)_2(OH)_3{\cdot}5H_2O$)[37] can be expressed by

$$\sigma = \frac{\mathrm{IAP}}{K_{sp}} - 1 = \mathrm{SI} - 1 \quad (1)$$

where IAP is the ion activity product and K_{sp} is its value at equilibrium (the solubility product for a Fe−P phase). This simulation is just an approximation as (i) the flow conditions in the AFM cell will most likely prevent equilibration with respect to goethite; (ii) any new phase could precipitate from a fluid layer at the interface in contact with the solid, while the bulk solution may remain undersaturated. The simulations performed represent the threshold thermodynamic limit for the process, that is, the equilibrium with respect to the substrate. An exact characterization of the saturation state of the solution from which the new formed phase precipitates is not possible with the experimental set up used in the present study.

The goethite structure is orthorhombic (unit cell a 4.59, b 9.94, c 3.02 Å, space group *Pbnm*) with perfect {010} cleavage faces (Figure 1A, B). The structure can be described in terms of double chains of edge-sharing octahedra running parallel to the [001] direction.[10] Figure 1C, D shows these chains are linked to adjacent double chains by corner-sharing with one chain and the OH groups are linked to another O atom in a chain diagonally opposite. The perfect cleavage on (010) is parallel to the approximately hexagonal close packed oxygen layers in the structure. The structure of the (010) goethite surface studied here has been described by Rakovan et al. (1999).[38]

RESULTS AND DISCUSSION

Dissolution of Goethite (010) Cleavage Surfaces. The AFM images of goethite surfaces exposed to $NH_4H_2PO_4$ solutions (5.0 mM, pH 4.5) confirm that dissolution occurs through a simple step retreat process by showing surfaces comprised of multiple straight-edged and non- straight steps without evidence of etch pit formation within the experimental time frame (Figure 2). On contact with reaction solutions for about 21 min, dissolution occurred with the removal of pre-existing steps with constant height (about 1.5 nm) (Figure 2C, F) from a flat surface. Note that these experiments used 10 mM NaCl solutions, that, as shown below, increase rates and probabilities of pit formation. We infer, therefore, that dissolution in $NH_4H_2PO_4$ solutions without background electrolytes also proceeds by simple step retreat. At conditions

DOI: 10.1021/acs.est.5b00312
Environ. Sci. Technol. 2015, 49, 4184−4192

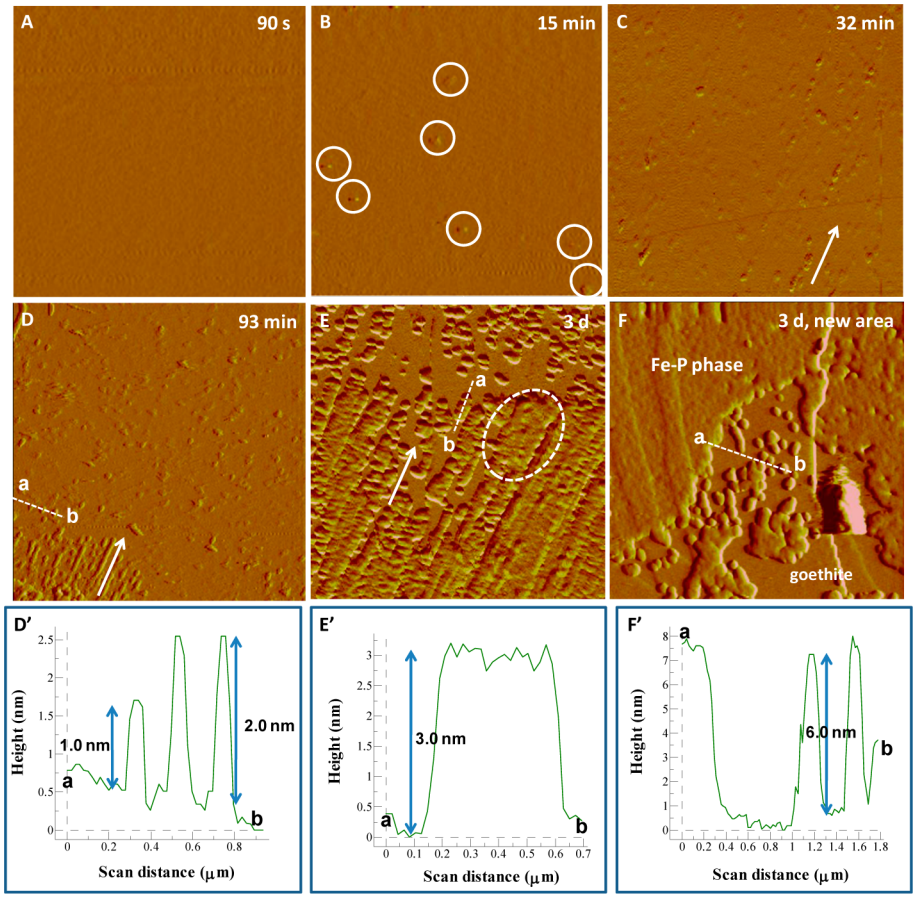

Figure 3. AFM time sequence (deflection images) showing in situ nucleation kinetics of Fe−P phases and the growth evolution of precipitates on a dissolving goethite surface in 50 mM $NH_4H_2PO_4$ (pH 4.5) at (A) t = 90 s, (B) 15 min, (C) 32 min and (D) 93 min, respectively. (E, F) Ex situ AFM images of the same goethite substrate as the above, reacting in solutions (50 mM $NH_4H_2PO_4$, pH 4.5) for 3 days at room temperature. Images A-F, 5 × 5 μm. (D′-F′) Height profile of the initially formed Fe−P nanoparticles (circled for clarity in (B)) and their developing growth on a goethite (010) cleavage face along section a → b (dashed lines in (D−F)). The average height of Fe−P nanoparticles is about 1.0−3.0 nm, that was almost unchanged in a short period (90 min) of reaction time. The growth of the nucleated particles led to the formation of 1-D short chains shown by arrows in (C, D) along the same orientation, and 2-D plates shown by a dotted ellipse in (E). Following a long period of reaction time (3 days), secondary particles formed (about 3.0−6.0 nm in height) shown in section a → b in (E, F). Finally, layering occurred (F).

where the driving force needed to initiate dissolution at dislocation defects is exceeded, our AFM observations reinforce the conclusion that the total dissolution rate is dominated by retreat of these preexisting steps and density of step edges.

Iron Phosphate Nucleation and Growth on Goethite (010) Cleavage Surfaces. The dissolution of goethite in the presence of all the experimental phosphate solutions provided a source of Fe^{3+} ions, which resulted in supersaturation of the interfacial fluid with respect to a Fe−P phase and its nucleation on the dissolving goethite surface. In situ AFM imaging demonstrated that the observed nanoparticles/nanoclusters were present partially as isolated entities with a height of 1.0−3.0 nm (Figure 3B−E) at the earliest nucleation stages or small spherical particles (about 6.0 nm in height) (Figure 3F) at the subsequent growth stages. A slow, diffusion-limited growth process is expected due to the reduction in the supply of Fe^{3+} ions from goethite surfaces as a result of the almost complete coverage of the reacting surface by the deposition of Fe−P plates (Figure 3F). The growth rate of Fe−P layers was not expected to drop to zero because some release of Fe ions from the noncovered areas of the dissolving goethite substrate (Figure 3F) still existed, and the thickness increased up to a final value of about 6.0 nm (Figure 3F′).

The growth of the nucleated particles led to the formation of one-dimensional short chains shown by arrows in Figure 3C and D along a specific direction. As shown in Figure 2, dissolution occurred by a simple retreat of preexisting steps with no evidence of forming etch pits on the exposed surfaces. The preferential chain-like alignments of nanoparticles may be related to the step orientation of the substrate, which is determined by the crystallographic orientation of the goethite. Moreover, these precipitates of nanoparticles were loosely attached at the initial stage and could be removed or realigned by scanning the AFM tip at higher contact force. The number of Fe−P nucleated nanoparticles increased with time for a given phosphate concentration, exhibiting a linear dependence with time. Faster nucleation rates were observed with increasing the $NH_4H_2PO_4$ solution concentration when the solution pH was kept constant (pH 4.5) (Figure 4A), whereas the nucleation rate decreased when the pH was raised to 6.0 at a constant concentration of 50 mM $NH_4H_2PO_4$ (Figure 4A and Supporting Information Figure S1). For a given $NH_4H_2PO_4$ concentration (50 mM, pH 4.5), faster nucleation rates were also observed with adding 10 mM $AlCl_3$ (Figure 4B and Supporting Information Figure S2). After 29 min, no further growth of nucleated crystals was observed. This could be

DOI: 10.1021/acs.est.5b00312
Environ. Sci. Technol. 2015, 49, 4184−4192

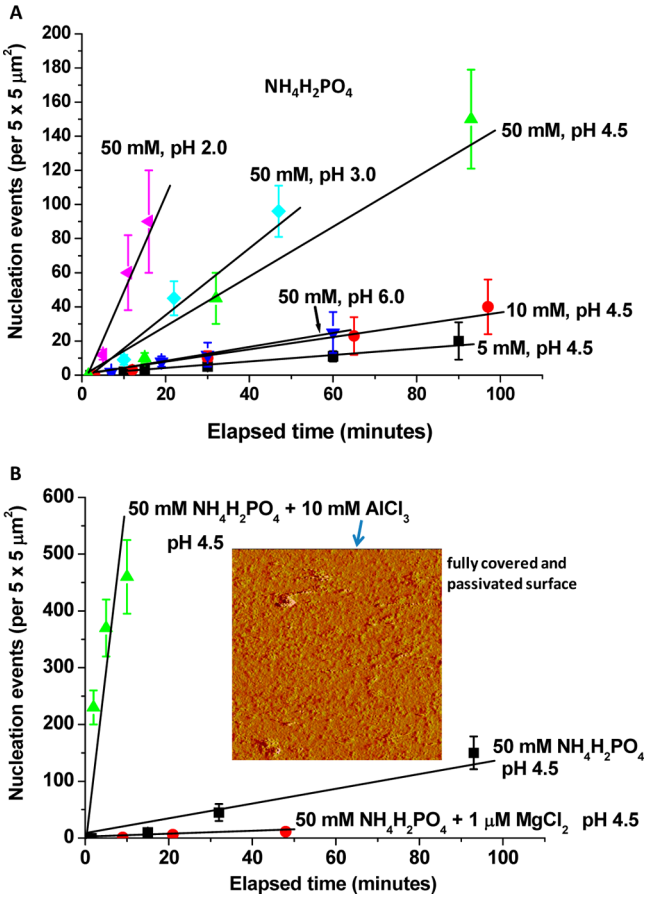

Figure 4. Kinetic analysis of surface nucleation of Fe−P phases on goethite substrates in short periods of reaction times. (A, B) Plot of time against different concentrations of $NH_4H_2PO_4$, pH values, and background electrolytes ($AlCl_3$ or $MgCl_2$), showing linear scaling of surface nucleation with time and dependence of the nucleation rate given by slopes of the lines (the solid line is a linear fit to the AFM data (the number of nucleated particles in a short time period)). Inset in (B) shows that after 29 min of injecting reaction solution (50 mM $NH_4H_2PO_4$ +10 mM $AlCl_3$, pH 4.5), the scan area (5 × 5 μm) was almost fully covered with the new nucleating particles, that passivated the reacting surface. Vertical error bars (the standard deviation of the mean) correspond to the variation in measured number of nucleated particles.

related to the fact that the goethite surface was rapidly covered by a layer of fine precipitates (Inset in Figure 4B), effectively passivating the surface so that no Fe^{3+} ions could be released to the interfacial fluid layer. Similar phenomena could be observed in the presence of various concentrations of NaCl (10 to 100 mM) (Supporting Information Figure S3). However, the nucleation rate significantly decreased when 1 μM $MgCl_2$ was added to the $NH_4H_2PO_4$ solution (50 mM, pH 4.5) (Figure 4B and Supporting Information Figure S4).

Upon input of a 50 mM $NH_4H_2PO_4$ solution in the presence of 10 μM citrate (pH 4.5), greater nucleation rates were observed than in the absence of citrate (Figure 5A−C). The rapid growth of the nucleated particles with different sizes (height) almost fully covered the goethite substrates in a short time period (32 min). When the citrate concentration was raised to 50 μM, the goethite dissolution was completely inhibited as no precipitation was seen under AFM (Figure 5D, E). Similar results have been shown in calcium phosphate growth on calcite surfaces.[5]

Identification of Surface Precipitates on Goethite (010) Cleavage Faces. After exposing cleaved goethite surfaces to 50 mM $NH_4H_2PO_4$ solutions (pH 4.5) for 3 days, the goethite surfaces were covered by layers and scattered particles of precipitates (Figures 6A). SEM-EDX analyses indicated these precipitates are composed of Fe, P, and O (Figure 6B). These precipitates formed on goethite (010) surfaces were also analyzed using Raman spectroscopy, however, no bands apart from those for goethite were detected most likely because the thickness of precipitates on the goethite substrates was too thin compared to the axial (depth) resolution of the Raman spectrometer which is typically on the order of a few microns.

Kinetics and Mechanisms of Coupled Dissolution and Precipitation Reactions at the Goethite-Phosphate Solution Interface. Depending on the chemical composition of the aqueous solution, the dissolution of even a few monolayers of a mineral surface can supersaturate a layer of solution at the mineral−fluid interface with respect to another solid phase, that subsequently may precipitate through an interface-coupled dissolution−precipitation mechanism.[39] The dissolution of goethite in the presence of all phosphate solutions provided a continuous source of Fe^{3+} ions, increasing the driving force SI at the solid−fluid interfacial layer, with respect to several Fe−P phases and eventually resulting in the nucleation and growth of a Fe−P phase on the dissolving goethite surface. Nucleation rates of the newly formed Fe−P phases are controlled by the solid−fluid interfacial energy and kinetic barriers related to desolvation, attachment, detachment, and diffusion.[40,41] Under the present conditions, we could not strictly separate thermodynamic and kinetic contributions to the control of the nucleation rate.

In general, iron oxides dissolve too slowly for in situ AFM study, even in the presence of step retreat (Figure 2), except under extreme conditions. In the absence of background electrolytes, the density of steps on the surface controls the rate at which a crystal dissolves. These steps can be preexisting on the initial crystal surface or at the crystal edges, emerge from dislocation sources, or be created by nucleating new vacancy islands.[42] In our experimental systems, no etch pits were observed, suggesting that the free energy barrier is too high for pit nucleation to occur on goethite on a time scale of our AFM experiments, and dissolution then is dominated by retreat of the preexisting steps as shown in Figure 2. For defect-free goethite surfaces (only preexisting straight-edged steps with no evidence of pitting, Figures 1 and 2) under far from equilibrium conditions (as is the case for our solutions), the dissolution rates increase with acidic pH (Supporting Information Figure S1).

There are several parallel dissolution pathways having different rate constants for goethite, including proton-promoted ($FeOOH + 3H^+ \rightarrow Fe(III)_{(aq)} + 2H_2O$, pH 2−3), ligand-promoted ($((FeOOH)>Fe^{III}-OH + L^- + H^+ \rightarrow (FeOOH)>Fe^{III}-L + H_2O \rightarrow FeOOH + Fe(III)-L_{(aq)}$, L^- = citrate, pH 4−6), reductive ($FeOOH + e^- + 3H^+ \rightarrow Fe(II)_{(aq)} + 2H_2O$), and synergistic. Goethite is regarded as an infinite *n*-mer extension of $[Fe_2(OH)_2]^{4+}$ (Figure 1C, D), and its dissolution is then a stepwise depolymerization.[43] Protons have the role of weakening bonds and thus increasing dissolution rates[44] and subsequent availability of Fe ions for Fe−P nucleation (Figure 4). Ligands binding as innersphere complexes to the surface groups of goethite increase dissolution rates, and the increase is proportional to the ligand surface concentration and the ligand

DOI: 10.1021/acs.est.5b00312
Environ. Sci. Technol. 2015, 49, 4184−4192

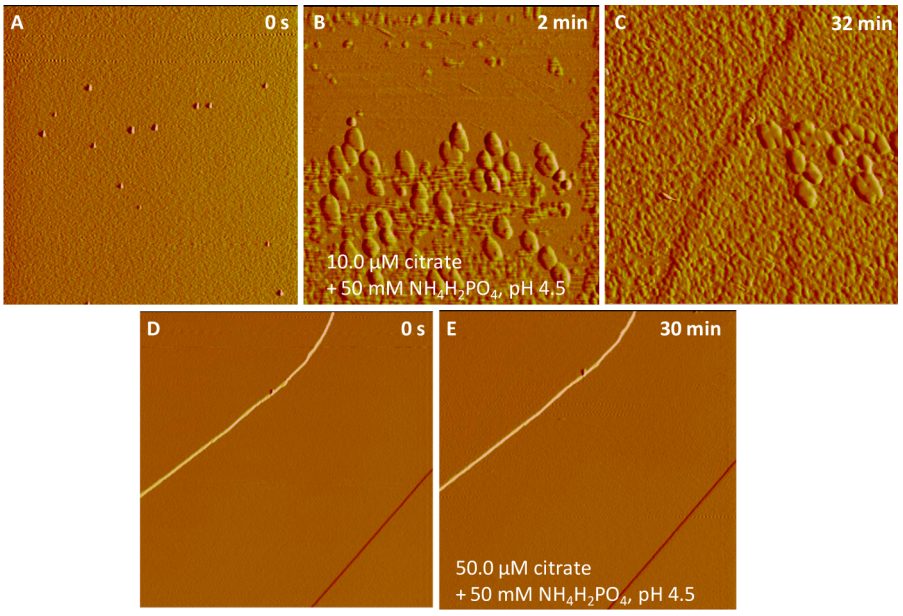

Figure 5. Density of nuclei formed on a goethite (010) surface at different times, from which nucleation kinetics of Fe−P phases can be determined in the presence of (A−C) 10.0 μM citrate and (D and E) 50 μM citrate with 50 mM $NH_4H_2PO_4$ at pH 4.5. AFM images A−E, 5 × 5 μm.

binding strength.[45−47] Fe cations bind much more strongly to oxygen-containing ligands[48,49] such as citrate. Two citrate-goethite surface complexes exhibit one protonated species at low pH, and one inner sphere complex prevailing at high pH and coordinated via a combination of hydroxyl and carboxylate groups.[48,49] In addition, an inner sphere complex involving only carboxylate coordination predominating at low pH has been identified.[50] Furthermore, ligands effective for promoting dissolution have two or more functional groups (carboxylate groups in citrate) capable of chelation to form innersphere bidentate mononuclear complexes. In contrast, ligands forming bidentate binuclear complexes may stabilize the surface against attack by H^+ and H_2O and thus inhibit the dissolution rate.

Under our experimental conditions, the major dissociated citrate species (H_2L^- at pH 4.5; acid dissociation constant of citrate: pK_{a1} = 3.13, pK_{a2} = 4.76, pK_{a3} = 6.40 at 298 K[49]) are likely to complex Fe to form low concentration Fe(citrate) (C) (log C = −7.03 M at citrate concentration of 50 μM, Supporting Information Table S4). The addition of citrate slightly decreases the *SI* of precipitating Fe−P minerals (Supporting Information Table S4) by the formation of Fe and P complexes in aqueous solution. An increase in the interfacial energy following the introduction of a high concentration of citrate (50 μM) may explain the observed inhibition of goethite dissolution and subsequent Fe−P precipitate formation on goethite (Figure 5D-E). At low concentrations (1−10 μM), the interaction of carboxyl groups of citrate with surface Fe^{3+} ions may increase the local concentration of a carboxylated additive in the vicinity of these cations,[51] thereby lowering the energy barrier for nucleation to promote the precipitation of Fe−P phases (Figure 5A−C). Moreover, carboxylate-containing molecules (citrate) may also reduce the magnitude of the diffusive barrier, E_K, by perturbations that displace water molecules. The result is a decrease in the energy barrier for attachment of solutes to the solid phase through cation desolvation.[52,53]

In the experiments aimed at determining the effect of background electrolytes on goethite dissolution, we adjusted the solution composition by adding $AlCl_3$ or NaCl or $MgCl_2$ to the 50 mM $NH_4H_2PO_4$ (pH 4.5) solution, which changed ionic strength. At the surface of goethite, two different types of reactive surface groups are present, that is, singly (≡FeOH(H)) and triply (≡Fe_3O(H)) coordinated oxygens.[54] The presence of salts will influence both aqueous speciation of goethite (Supporting Information Tables S1−3) and the phosphate primary speciation ($H_2PO_4^-$ and H_3PO_4 at pH 4.5) adsorbed on goethite, which determine the goethite dissolution rates. Moreover, electrolyte ions like Na^+, Cl^- or Mg^{2+} may change the charge distribution in the inner and outer Stern layer by ion-specific weak interactions, that is, ion pair formation.[55] A different electrostatic interaction of the cations with the proton charge at the goethite surface would occur. The effect is stronger for the divalent cations like Mg^{2+} than for the monovalent ions such as Na^+. The modeling revealed that Mg^{2+} is mainly adsorbed as a bidentate innersphere complex by the combination of a $FeOH^{-1/2}$ and a $Fe_3O^{-1/2}$ surface group.[55] Furthermore, natural Fe(III) (hydr)oxides contain numerous impurities such as Al^{3+},[56] which is a common and abundant element in acid soils. Hu et al.[57] also showed that Al^{3+} ions affected the amount of water included in ferrihydrite, although the water lost was thought to be due to Ostwald ripening.

Calculated SI values show that it could be thermodynamically favorable for more than one iron phosphate phase to precipitate if equilibrium were reached with respect to goethite. The three most likely Fe-phosphate phases are cacoxenite, tinticite, and strengite, the former (cacoxenite) being more favorable because of its higher SI in all the experimental solutions (Supporing Information Tables S1−S4). Saturation indices of possible Fe−P phases including strengite, tinticite, and cacoxenite in the presence of 50 mM $NH_4H_2PO_4$ solution at pH 4.5 are 1.4, 19.8, and 28.2, respectively. Following the addition of 100 mM NaCl into 50 mM $NH_4H_2PO_4$ solution at pH 4.5, SI with respect to strengite, tinticite and cacoxenite at the equilibrium with goethite would slightly raise to 1.5, 19.9, and 28.4, respectively. However, as pH was decreased to 2.0 from 4.5 in 50 mM $NH_4H_2PO_4$ solution (pH 4.5), *SI* with respect to strengite,

DOI: 10.1021/acs.est.5b00312
Environ. Sci. Technol. 2015, 49, 4184−4192

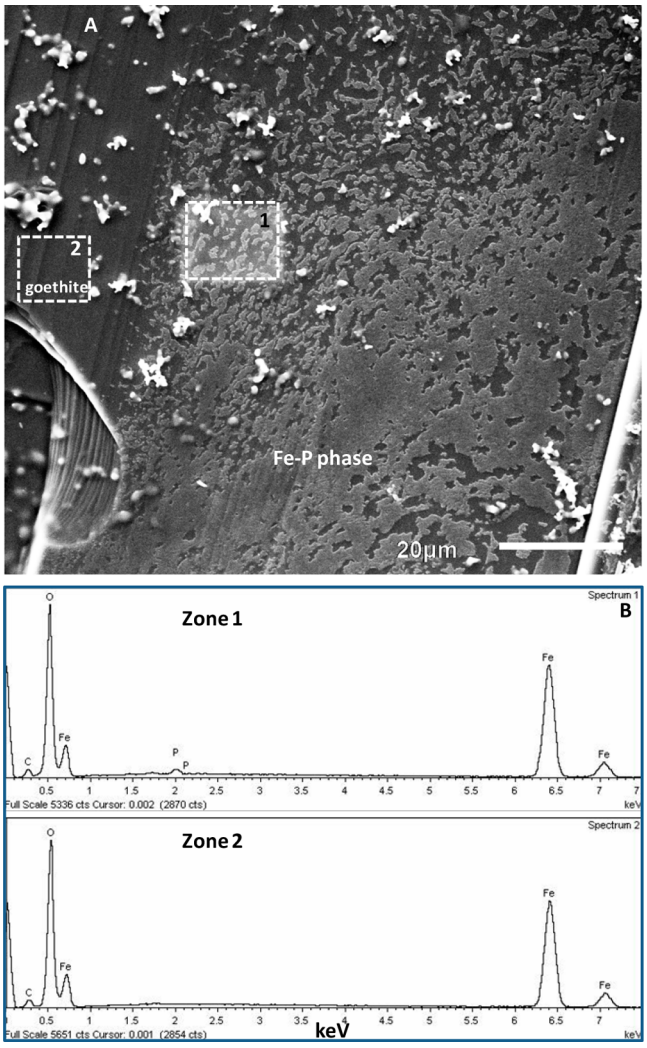

Figure 6. (A) SEM image showing the ex situ formation of Fe−P precipitates on goethite after 3 days of interfacial reaction in a 50 mM $NH_4H_2PO_4$ (pH 4.5) solution. The goethite substrate was almost fully covered with the layer of precipitates. The dotted rectangles indicate zones chosen for EDX analyses. The brighter contrast of zone 1 resulted from an earlier scan indicating that the surface was sensitive to the electron beam. (B) EDX spectra taken from zone 1 and 2 shown by dotted rectangles in (A), indicating an iron phosphate phase and goethite substrate, respectively.

tinticite and cacoxenite would significantly raise to 3.5, 23.9, and 34.4, respectively (Supporting Information Table S1). The simulation results show an obvious increase in aqueous phosphate including $FeHPO_4^+$, $FeH_2PO_4^{+2}$ and $FeH_2PO_4^+$ by increasing aqueous speciation concentrations of Fe^{3+} and $FeOH^{+2}$ (Supporting Information Table S1) as the pH decreases to 2.0 from 4.5 to induce a rapid goethite dissolution (Supporting Information Figure S1). Moreover, our AFM observations show that faster Fe−P nucleation rates are achieved with increasing ionic strength by adding NaCl or $AlCl_3$, and that the goethite surface is rapidly covered and subsequently passivated by a layer of fine precipitates (Figure 4 and Supporting Information Figures S2 and S3). Surface coverage by the new Fe−P phase should not armor the goethite from further reaction; the newly forming precipitate layer must have porosity and hence permeability to allow continued fluid access to the parent phase.[39] The new phase is more stable than goethite (and hence less soluble in the soil solutions), meaning that more goethite is dissolved than product precipitated within the same external dimensions.[39,58]

The dependence of mineral dissolution rates is complex, and a further complication occurs in the presence of background electrolytes. Dove et al.[42] have suggested that the "salt effect" (dissolution rate enhancement by the major cationic solutes) arises from a crossover in dominant nucleation mechanism to greatly increase step density. In the present study, the AFM images do not allow us to determine whether this transition is present as NaCl or $AlCl_3$ is added to $NH_4H_2PO_4$ solution. Previous AFM studies have demonstrated that the presence of background electrolytes enhances the calcite dissolution rate,[34] and the magnitude of this enhancement is determined by the nature and concentration of the electrolytes, possibly through modifying water structure dynamics as well as solute and surface hydration.[59] In addition to the influence of the ionic strength, aluminum species have a high affinity for P and at pH 4.5, AlOHP species (nanoprecipitates) may form in solution and be adsorbed on the surfaces of goethite; the effect of changing the concentrations of Al^{3+} ions (primary speciation including Al^{3+} and $AlOH^{+2}$ in 50 mM $NH_4H_2PO_4$ solutions at pH 4.5), which is a key reactant to forming Al-substituted cacoxenite ($Fe^{3+}{}_{24}Al(PO_4)_{17}O_6(OH)_{12}\cdot 17H_2O$) or wavellite ($Al_3(PO_4)_2(OH)_3\cdot 5H_2O$) (Supporting Information Table S2), may be much more significant than that of ionic strength. This suggests that a continuum of processes may be coexisting, from adsorption (inner-sphere complexes) to precipitation to solid-phase transformation. However, in the present study the nature of initially formed precipitates (crystalline or noncrystalline/amorphous or coexistence) still remains unknown.

As shown in Figure 4 and Supporting Information Figure S4, in the presence of low concentration Mg^{2+} ions (1 μM) in 50 mM $NH_4H_2PO_4$ solutions (pH 4.5), the Fe−P nucleation was significantly inhibited when compared to its absence. The quantitative AFM analyses have shown that Mg^{2+} inhibits etch pit spreading, although it also increases the density and depth of etch pits nucleated on calcite surfaces.[60] Therefore, we suggest for the present observation that Mg^{2+} may inhibit the retreat of the preexisting steps on goethite, but the free energy barrier to initiate a pit or dislocation on a perfect goethite surface is high, thus the overall dissolution rate and subsequent Fe−P nucleation rate are lowered (Supporting Information Figure S4). Furthermore, phosphate is adsorbed preferentially as protonated species at low pH and high surface coverage;[15,61] that involves a ligand exchange reaction, and a Fe−O(H) bond is broken and a new Fe−O−P bond is formed. Three surface species have been described for the adsorption behavior of phosphate on goethite, that is, a monodentate $\equiv FeOPO_3$, a bidentate $\equiv(FeO)_2PO_2$, and a protonated bidentate $\equiv(FeO)_2POOH$ species.[18,62,63] Kim et al.[26] suggested the most reactive sites for phosphate adsorption on each FeOOH polymorph. For the competitive adsorption of cations such as Mg^{2+} and phosphate on goethite, modeling has shown the formation of both $\equiv(FeOH)_2Mg$ and $\equiv(FeOH)_2MgOH$.[64] Thus, their formation may inhibit phosphate adsorption and subsequent Fe−P nucleation.

To summarize, the distribution of phosphate at the goethite−water interface is dependent on the solution composition, including the activity of phosphate species, pH and ionic strength, thereby influencing phosphate availability. Based on the present study, we predict a significant decrease in the dissolved phosphate concentration of the soil solution due

DOI: 10.1021/acs.est.5b00312
Environ. Sci. Technol. 2015, 49, 4184−4192

to increased phosphate adsorption and the corresponding precipitation on goethite mineral surfaces at elevated phosphate concentrations and low pH. The bioavailability of phosphate will be rapidly reduced at high $NaCl/AlCl_3$ concentrations at the earlier stages of P application. Following the goethite surface passivation by this rapid Fe−P nucleation, phosphate immobilization will be inhibited, and the presence of Mg^{2+} ions will exert a further inhibition. Furthermore, concentrations of organic acids such as citrate in the bulk soil solution typically range from 0.1 μM to 0.1 mM,[65] and the mean citrate concentration in the rhizosphere is higher than the concentration, 50 μM, used in our AFM experiments. The presence of citrate can increase P availability by suppressing crystallization of Fe−P phases such as cacoxenite.

Goethite in surface environments is generally present as reactive nanoparticles, probably in equilibrium with interacting solution where sorption processes are mainly dominant (adsorption and/or chemisorption). However, in many instances, when phosphate fertilizers are applied to soil, a substantial disequilibrium situation that will drive goethite dissolution and phosphate precipitation may occur. Therefore, sorption processes may play a less important role; our present results provide an alternative understanding of goethite mineral surface-induced Fe−P precipitation, with possible implications for the management of phosphate immobilization in goethite-rich soils and phosphate-induced eutrophication in water bodies.

■ ASSOCIATED CONTENT

Supporting Information

Aqueous speciation of goethite and saturation indices (SI) with respect to different Fe−P phases (Tables S1−4); AFM images of goethite surface under various reaction conditions (Figures S1−4). This material is available free of charge via the Internet at http://pubs.acs.org.

■ AUTHOR INFORMATION

Corresponding Authors

* (L.W.) Phone/fax: +86-27-87288095; e-mail: ljwang@mail.hzau.edu.cn.
*(C.V.P.) Phone: +49-251-8333454; fax: +49-251-8338397; e-mail: putnisc@uni-muenster.de.

Notes

The authors declare no competing financial interest.

■ ACKNOWLEDGMENTS

This work was supported by the National Natural Science Foundation of China (41471245, 41071208), a Specialized Research Fund for the Doctoral Program of Higher Education (20130146110030), and the Fundamental Research Funds for the Central Universities (2012MBDX014) (to L. J. W.). E. Ruiz-Agudo acknowledges funding from the Spanish Government (Grant MAT2012-37584-ERDF funds) and the Junta de Andalucía (research group RNM-179 and project P11-RNM-7550), as well as the receipt of a Ramón y Cajal grant from the Spanish Government (Ministerio de Economia y Competitividad). C.V. Putnis and A. Putnis acknowledge support through EU Marie Curie initial training networks (FlowTrans, CO_2 React and Minsc).

■ REFERENCES

(1) Filippelli, G. M. The global phosphorous cycle: Past, present, and future. *Elements* **2008**, *4*, 89−95.
(2) Gilbert, N. The disappearing nutrient. *Nature* **2009**, *461*, 716−718.
(3) Conley, D. J.; Paerl, H. W.; Howarth, R. W.; Boesch, D. F.; Seitzinger, S. P.; Havens, K. E.; Lancelot, C.; Likens, G. E. Controlling eutrophication: Nitrogen and phosphorus. *Science* **2009**, *323*, 1014−1015.
(4) Elser, J. A broken biogeochemical cycle. *Nature* **2011**, *478*, 29−31.
(5) Wang, L. J.; Ruiz-Agudo, E.; Putnis, C. V.; Menneken, M.; Putnis, A. Kinetics of calcium phosphate nucleation and growth on calcite: Implications for predicting the fate of dissolved phosphate species in alkaline soils. *Environ. Sci. Technol.* **2012**, *46*, 834−842.
(6) Bromfield, S. M. Relative contribution of iron and aluminium in phosphate sorption by acid surface soils. *Nature* **1964**, *201*, 321−322.
(7) Shen, J. B.; Yuan, L.; Zhang, J. L.; Li, H.; Bai, Z.; Chen, X.; Zhang, W.; Zhang, F. S. Phosphorus dynamics: From soil to plant. *Plant Physiol.* **2011**, *156*, 997−1005.
(8) Kaplan, D. I.; Knox, A. S. Enhanced contaminant desorption induced by phosphate mineral additions to sediment. *Environ. Sci. Technol.* **2004**, *38*, 3153−3160.
(9) Schwertmann, U.; Taylor, R. M. *Iron Oxides. In Minerals in Soil Environments*; Soil Science Society of America: Madison, WI, 1990; Vol. *1*. p379−439.
(10) Cornell, R. M.; Schwertmann, U. *The Iron Oxides: Structure, Properties, Reactions, Occurrence and Uses*, 2nd ed.; Wiley-VCH: Weinheim, Germany, 2003.
(11) Torrent, J. Interactions between phosphate and iron oxide. *Adv. GeoEcol.* **1997**, *30*, 321−344.
(12) Weng, L. P.; Vega, F. A.; Van Riemsdijk, W. H. Competitive and synergistic effects in pH dependent phosphate adsorption in soils: LCD modeling. *Environ. Sci. Technol.* **2011**, *45*, 8420−8428.
(13) Liu, H.; Chen, T.; Frost, R. L. An overview of the role of goethite surfaces in the environment. *Chemosphere* **2014**, *103*, 1−11.
(14) Atkinson, R. J.; Posner, A. M.; Quirk, J. P. Kinetics of isotopic exchange of phosphate at the α-FeOOH−aqueous solution interface. *J. Inorg. Nucl. Chem.* **1972**, *34*, 2201−2211.
(15) Tejedor-Tejedor, M. I.; Anderson, M. A. The protonation of phosphate on the surface of goethite as studied by CIR-FTIR and electrophoretic mobility. *Langmuir* **1990**, *6*, 602−611.
(16) Torrent, J.; Schwertmann, U.; Barron, V. Fast and slow phosphate sorption by goethite-rich natural materials. *Clays Clay Miner.* **1992**, *40*, 14−21.
(17) Strauss, R.; Brumer, G. W.; Barrow, N. J. Effects of crystallinity of goethite: II. Rates of sorption and desorption of phosphate. *Eur. J. Soil Sci.* **1997**, *48*, 101−114.
(18) Geelhoed, J. S.; Hiemstra, T.; Van Riemsdijk, W. H. Phosphate and sulfate adsorption on goethite: Single anion and competitive adsorption. *Geochim. Cosmochim. Acta* **1997**, *61*, 2389−2396.
(19) Fendorf, S.; Eick, M. J.; Grossl, P.; Sparks, D. L. Arsenate and chromate retention mechanisms on goethite. 1. Surface structure. *Environ. Sci. Technol.* **1997**, *31*, 315−320.
(20) Nowack, B.; Stone, A. T. Adsorption of phosphonates onto the goethite−water interface. *J. Colloid Interface Sci.* **1999**, *214*, 20−30.
(21) Lin, S. H.; Kao, H. C.; Cheng, C. H.; Juang, R. S. An EXAFS study of the structures of copper and phosphate sorbed onto goethite. *Colloids Surf., A* **2004**, *234*, 71−75.
(22) Kwon, K. D.; Kubicki, J. D. Molecular orbital theory study on surface complex structures of phosphates to iron hydroxides: Calculation of vibrational frequencies and adsorption energies. *Langmuir* **2004**, *20*, 9249−9254.
(23) Khare, N.; Hesterberg, D.; Martin, J. D. XANES investigation of phosphate sorption in single and binary systems of iron and aluminum oxide minerals. *Environ. Sci. Technol.* **2005**, *39*, 2152−2160.
(24) Villalobos, M.; Perez-Gallegos, A. Goethite surface reactivity: A macroscopic investigation unifying proton, chromate, carbonate, and lead (II) adsorption. *J. Colloid Interface Sci.* **2008**, *326*, 307−323.

DOI: 10.1021/acs.est.5b00312
Environ. Sci. Technol. 2015, 49, 4184−4192

(25) Rahnemaie, R.; Hiemstra, T.; van Riemsdijk, W. H. Geometry, charge distribution, and surface speciation of phosphate on goethite. *Langmuir* **2007**, *23*, 3680−3689.
(26) Kim, J.; Li, W.; Philips, B. L.; Grey, C. P. Phosphate adsorption on the iron oxyhydroxides goethite, akaganeite, and lepidocrocite: A ^{31}P NMR study. *Energy Environ. Sci.* **2011**, *4*, 4298−4305.
(27) Arai, Y.; Sparks, D. L. ATR-FTIR spectroscopic investigation on phosphate adsorption mechanisms at the ferrihydrite-water interface. *J. Colloid Interface Sci.* **2001**, *241*, 317−326.
(28) Luengo, C.; Brigante, M.; Antelo, J.; Avena, M. Kinetics of phosphate adsorption on goethite: Comparing batch adsorption and ATR-IR measurements. *J. Colloid Interface Sci.* **2006**, *300*, 511−518.
(29) Chitrakar, R.; Tezuka, S.; Sonoda, A.; Sakane, K.; Ooi, K.; Hirotsu, T. Phosphate adsorption on synthetic goethite and akaganeite. *J. Colloid Interface Sci.* **2006**, *298*, 602−608.
(30) Jonasson, R. G.; Martin, R. R.; Giuliacci, M. E.; Tazaki, K. Surface reactions of goethite with phosphate. *J. Chem. Soc. Faraday Trans.* **1988**, *1*, 2311.
(31) Li, L.; Stanforth, R. Distinguishing adsorption and surface precipitation of phosphate on goethite (a-FeOOH). *J. Colloid Interface Sci.* **2000**, *230*, 12−21.
(32) Ler, A.; Stanforth, R. Evidence for surface precipitation of phosphate on goethite. *Environ. Sci. Technol.* **2003**, *37*, 2694−2700.
(33) Nooney, M. G.; Campbell, A.; Murrell, T. S.; Lin, X.; Hossner, L. R.; Chusuei, C.; Goodman, D. W. Nucleation and growth of pahosphate on metal oxide thin films. *Langmuir* **1998**, *14*, 2750−2755.
(34) Ruiz-Agudo, E.; Kowacz, M.; Putnis, C. V.; Putnis, A. The role of background electrolytes on the kinetics and mechanism of calcite dissolution. *Geochim. Cosmochim. Acta* **2010**, *74*, 1256−1267.
(35) Parkhurst, D. L.; Appelo, C. A. J. *Users guide to PHREEQC-(version 2). A Computer Program for Speciation, Batch Reaction, One-Dimensional Transport, and Inverse Geochemical Calculations*, U.S. Geological Survey Water-resources Investigations Report, 1999; pp 99−4259.
(36) Nriagu, J. O.; Dell, C. I. Diagenetic formation of iron phosphates in recent lake sediments. *Am. Mineral.* **1974**, *59*, 934−946.
(37) Vieillard, P.; Tardy, Y. Stability fields of clays and aluminum phosphates: Parageneses in lateritic weathering of argillaceous phosphatic sediments. *Am. Mineral.* **1979**, *64*, 626−634.
(38) Rakovan, J.; Becker, U.; Hochella, M. F. Aspects of goethite surface microtopography, structure, chemistry, and reactivity. *Am. Mineral.* **1999**, *84*, 884−894.
(39) Putnis, A. Why mineral interfaces matter. *Science* **2014**, *343*, 1441−1442.
(40) Chernov, A. A. *Modern Crystallography III: Crystal Growth*; Springer: Berlin, 1984; pp 48−103.
(41) Giuffre, A. J.; Hamm, L. M.; Han, N.; De Yoreo, J. J.; Dove, P. M. Polysaccharide chemistry regulates kinetics of calcite nucleation through competition of interfacial energies. *Proc. Natl. Acad. Sci. U.S.A.* **2013**, *110*, 9261−9266.
(42) Dove, P. M.; Han, N.; De Yoreo, J. J. Mechanisms of classical crystal growth theory explain quartz and silicate dissolution behavior. *Proc. Natl. Acad. Sci. U.S.A.* **2005**, *102*, 15357−15362.
(43) Zinder, B.; Furrer, G.; Stumm, W. The coordination chemistry of weathering. 2. Dissolution of Fe(III) oxides. *Geochim. Cosmochim. Acta* **1986**, *50*, 1861−1869.
(44) Stumm, W. Reactivity at the mineral-water interface: Dissolution and inhibition. *Colloids Surf., A* **1997**, *120*, 143−166.
(45) Stone, A. T.; Torrents, A.; Smolen, J.; Vasudevan, D.; Hadley, J. Adsorption of organic compounds possessing ligand donor groups at the oxide/water interface. *Environ. Sci. Technol.* **1993**, *27*, 895.
(46) Duckworth, O. W.; Martin, S. T. Surface complexation and dissolution of hematite by C1-C6 dicarboxylic acids at pH = 5.0. *Geochim. Cosmochim. Acta* **2001**, *65*, 4289−4301.
(47) Reichard, P. U.; Kretzschmar, R.; Kraemer, S. M. Dissolution mechanisms of goethite in the presence of siderophores and organic acids. *Geochim. Cosmochim. Acta* **2007**, *71*, 5635−5650.
(48) Martin, S. T. Precipitation and dissolution of iron and manganese oxides, Chapter 3. In *Environmental Catalysis*; Vicki H. Grassian, Ed.; CRC Press: Boca Raton, FL, 2005; pp 61−81.
(49) Mudunkotuwa, I. A.; Grassian, V. H. Citric acid adsorption on TiO_2 nanoparticles in aqueous suspensions at acidic and circumneutral pH: Surface coverage, surface speciation, and its impact on nanoparticle−nanoparticle interactions. *J. Am. Chem. Soc.* **2010**, *132*, 14986−14994.
(50) Lindegren, M.; Loring, J. S.; Persson, P. Moleuclar structures of citrate and tricarballylate adsorbed on α-FeOOH particles in aqueous suspensions. *Langmuir* **2009**, *25*, 10639−10647.
(51) Mann, S.; Archibald, D. D.; Didymus, J. M.; Douglas, T.; Heywood, B. R.; Meldrum, F. C.; Reeves, N. J. Crystallization at inorganic-organic interfaces: Biominerals and biomimetic synthesis. *Science* **1993**, *261*, 1286−1292.
(52) Elhadj, S.; De Yoreo, J. J.; Hoyer, J. R.; Dove, P. M. Role of molecular charge and hydrophilicity in regulating the kinetics of crystal growth. *Proc. Natl. Acad. Sci. U.S.A.* **2006**, *103*, 19237−19242.
(53) Piana, S.; Jones, F.; Gale, J. D. Aspartic acid as a crystal growth catalyst. *CrystEngComm* **2007**, *9*, 1187−1191.
(54) Hiemstra, T.; Venema, P.; van Riemsdijk, W. H. Intrinsic proteon affinity of reactive surface groups of metal (hydr)oxides: The bond valence principle. *J. Colloid Interface Sci.* **1996**, *184*, 680−692.
(55) Rahnemaie, R.; Hiemstra, T.; van Riemsdijk, W. H. Inner- and outer-sphere complexation of ions at the goethite-solution interface. *J. Colloid Interface Sci.* **2006**, *297*, 379−388.
(56) Bazilevskaya, E.; Archibald, D. D.; Aryanpour, M.; Kubicki, J. D.; Martinez, C. E. Aluminum coprecipitates with Fe (hydr)oxides: Does isomorphous substitution of Al^{3+} for Fe^{3+} in goethite occur? *Geochim. Cosmochim. Acta* **2011**, *75*, 4667−4683.
(57) Hu, Y.; Li, Q.; Lee, B.; Jun, Y. S. Aluminum affects heterogeneous Fe(III) (hydr)oxide nucleation, growth, and Ostwald ripening. *Environ. Sci. Technol.* **2014**, *48*, 299−306.
(58) Putnis, C. V.; Ruiz-Agudo, E. The mineral-water interface: Where minerals react with the environment. *Elements* **2013**, *9*, 177−182.
(59) Stack, A. G. Molecular dynamics simulations of solvation and kink site formation at the {001} Barite-water interface. *J. Phys. Chem. C* **2009**, *113*, 2104−2110.
(60) Ruiz-Agudo, E.; Putnis, C. V.; Jimenez-Lopez, C.; Rodriguez-Navarro, C. An atomic force microscopy study of calcite dissolution in saline solutions: The role of magnesium ions. *Geochim. Cosmochim. Acta* **2009**, *73*, 3201−3217.
(61) Persson, P.; Nilsson, N.; Sjoberg, S. Structure and bonding of orthophosphate ions at the iron oxide-aqueous interface. *J. Colloid Interface Sci.* **1996**, *177*, 263−275.
(62) Geelhoed, J. S.; Hiemstra, T.; van Riemsdijk, W. H. Competitive interaction between phosphate and citrate on goethite. *Environ. Sci. Technol.* **1998**, *32*, 2119−2123.
(63) Antelo, J.; Avena, M.; Fiol, S.; Lopez, R.; Arce, F. Effects of pH and ionic strength on the adsorption of phosphateand arsenate at the goethite−water interface. *J. Colloid Interface Sci.* **2005**, *285*, 476−486.
(64) Stachowicz, M.; Hiemstra, T.; van Riemsdijk, W. H. Multi-competitive interaction of As(III) and As (V) oxyanions with Ca^{2+}, Mg^{2+}, PO_4^{3-}, and CO_3^{2-} ions on goethite. *J. Colloid Interface Sci.* **2008**, *320*, 400−414.
(65) Qin, L. H.; Zhang, W. J.; Lu, J. W.; Stack, A. G.; Wang, L. J. Direct imaging of nanoscale dissolution of dicalcium phosphate dihydrate by an organic ligand: Concentration matters. *Environ. Sci. Technol.* **2013**, *47*, 13365−13374.

DOI: 10.1021/acs.est.5b00312
Environ. Sci. Technol. 2015, 49, 4184−4192